Computational identification of a metal organic framework for high selectivity membrane-based CO2/CH4 separations: Cu(hfipbb)(H2hfipbb)0.5

ARTICLE *in* PHYSICAL CHEMISTRY CHEMICAL PHYSICS · DECEMBER 2009

Impact Factor: 4.49 · DOI: 10.1039/b918254n · Source: PubMed

4 AUTHORS, INCLUDING:

Taku Watanabe
Samsung R&D Institute Japan
23 PUBLICATIONS **638** CITATIONS
SEE PROFILE

Seda Keskin
Koc University
69 PUBLICATIONS **1,949** CITATIONS
SEE PROFILE

Computational identification of a metal organic framework for high selectivity membrane-based CO_2/CH_4 separations: $Cu(hfipbb)(H_2hfipbb)_{0.5}$

Taku Watanabe, Seda Keskin, Sankar Nair and David S. Sholl*

Received 3rd September 2009, Accepted 8th October 2009
First published as an Advance Article on the web 29th October 2009
DOI: 10.1039/b918254n

The identification of membrane materials with high selectivity for CO_2/CH_4 mixtures could revolutionize this industrially important separation. We predict using computational methods that a metal organic framework (MOF), $Cu(hfipbb)(H_2hfipbb)_{0.5}$, has unprecedented selectivity for membrane-based separation of CO_2/CH_4 mixtures. Our calculations combine molecular dynamics, transition state theory, and plane wave DFT calculations to assess the importance of framework flexibility in the MOF during molecular diffusion. This combination of methods should also make it possible to identify other MOFs with attractive properties for kinetic separations.

Efficient separation of CO_2 from CH_4 is an important issue in natural gas processing[1,2] and landfill gas recovery.[3] Enormous reserves of natural gas with high levels of CO_2 are known.[4,5] Before these resources can be used, robust methods to purify CH_4 from CH_4/CO_2 mixtures with low cost are required. Membranes offer a powerful general approach to this challenge, provided that robust materials with high selectivities can be identified.[6]

Metal organic frameworks (MOFs) are a class of crystalline nanoporous materials that have many potential advantages over traditional nanoporous materials for adsorption and chemical separations. An enormous number of different MOFs are known[7,8] and the physical and chemical structures of the pores in MOFs can be tuned with relative ease during synthesis. A range of experimental and modeling studies have examined MOFs in adsorption-based separations,[9–12] while a smaller group of studies has examined MOF membranes.[13–16] In MOFs, as in most nanoporous materials, CO_2 adsorbs more strongly than CH_4, although in general the selectivities that have been achieved based on adsorption are not dramatically different from those in other nanoporous materials such as zeolites. Because the pores of many MOFs are large relative to CO_2 and CH_4 molecules, diffusion of CO_2 is typically slower than CH_4. In MOFs of this kind, membrane-based separations, which rely on a combination of adsorption selectivity and diffusion selectivity, would have lower selectivity than an adsorption-based separation.[17]

The conflicting trends in adsorption and diffusion selectivity noted above are not a universal property of all nanoporous materials. The silica zeolite DDR has been shown to have very high selectivity for CO_2 from CO_2/CH_4 mixtures when used as a membrane.[18,19] Molecular modeling of DDR demonstrated that this zeolite has two crucial properties that make this kinetic-based separation possible.[18] First, molecular diffusion of CO_2 is far more rapid than CH_4 in DDR because diffusion is controlled by narrow windows that restrict the motion of CH_4 to a much greater extent than the slightly smaller CO_2 molecules. Second, the pores between these windows are large relative to both molecules, so the presence of the slowly diffusing CH_4 does not significantly impede the motion of CO_2. The same two principles apply to a small number of other zeolites and aluminophosphates.[20,21]

In this paper, we show using computational modeling that the structural features that make DDR and SAPO-34 appealing materials for CO_2/CH_4 separations are also shared by a microporous MOF, $Cu(hfipbb)(H_2hfipbb)_{0.5}$ ($H_2hfipbb$ = 4,4′-(hexafluoroisopropylidene) bis(benzoic acid)). We use molecular simulations to examine the adsorption and diffusion of CO_2 and CH_4 in this MOF, both as single components and as mixtures. These simulations suggest that the CH_4 diffusion through $Cu(hfipbb)(H_2hfipbb)_{0.5}$ is strongly hindered by large energy barriers created by narrow windows in the MOF's pores. Because the effects of structural relaxation in these windows could potentially be significant, we supplement our molecular simulations with quantum chemistry calculations using plane wave density functional theory (DFT). Our DFT calculations use the full periodic crystal structure of the MOF. Aside from the intrinsic significance of identifying a new material for this industrially important separation, the suite of methods we apply here will be applicable to a broad class of MOFs. They therefore open the possibility of efficiently identifying other MOFs among the thousands of known MOFs for use in high performance kinetic separations.

$Cu(hfipbb)(H_2hfipbb)_{0.5}$ is a crystalline interpenetrating framework containing ordered microporous 1D channels, built on a $Cu_2(hfipbb)_4(H_2hfipbb)_2$ paddle-wheel building unit (see Fig. 1). Its synthesis, structure and room temperature adsorption properties for H_2 and selected alkanes have been examined experimentally.[22–24] We selected this MOF because it has cages that are moderate in size relative to small gas molecules ($\sim$5.1 $\times$ 5.1 Å) connected by small windows ($\sim$3.5 $\times$ 3.2 Å) based on atom to atom distances in the reported crystal structure.[22] Pan *et al.* examined propane, butane and pentane adsorption in $Cu(hfipbb)(H_2hfipbb)_{0.5}$, showing that this adsorption is size selective because of the favorable match between the larger of these alkanes and the material's cages.[24] Similar effects are known for size selective adsorption in zeolites.[25] These experiments show that alkanes,

School of Chemical & Biomolecular Engineering, Georgia Institute of Technology, Atlanta GA, 30332-0100, USA.
E-mail: david.sholl@chbe.gatech.edu

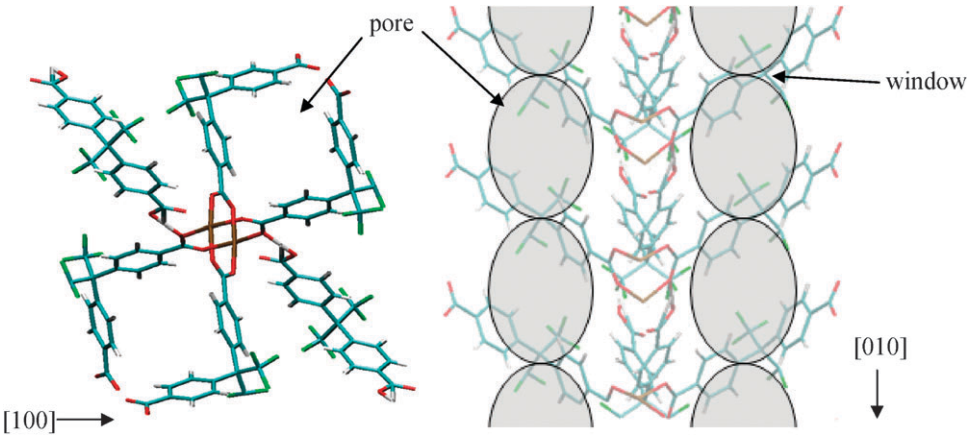

Fig. 1 Structure of Cu(hfipbb)(H_2hfipbb)$_{0.5}$ in [010] direction (left) and [10-1] direction (right). The right structure schematically shows the locations of the one-dimensional channels available for molecular adsorption and diffusion.

including CH_4, can adsorb in Cu(hfipbb)(H_2hfipbb)$_{0.5}$, but no information is available regarding the diffusivities of these adsorbed molecules. We know of no previous reports of adsorption or diffusion of CO_2 in this material.

Molecular simulation methods for modeling gas adsorption and diffusion in MOFs are now quite well established, as described in a recent review.[12] We performed adsorption and diffusion simulations of CO_2/CH_4 mixtures in Cu(hfipbb)-(H_2hfipbb)$_{0.5}$ using grand canonical Monte Carlo (GCMC) and equilibrium molecular dynamics (EMD), respectively. All simulations were performed at room temperature using a rigid MOF structure with atomic positions obtained from experimental data.[22] A simulation volume of $2 \times 2 \times 2$ crystallographic unit cells was used for all simulations. Assuming that the MOF is rigid greatly reduces the complexity of defining interatomic potentials for these simulations, as well as their computational efficiency. Later, we use plane wave DFT calculations to assess whether this assumption is justified.

Methane was modeled as a spherical Lennard-Jones (LJ) particle, while CO_2 was modeled as a rigid three-site molecule using the EPM2 model, an all atom model with LJ potentials and atomic charges to approximate the quadrupole moment of CO_2.[26,27] The Lorentz-Berthelot mixing rules were employed to calculate the adsorbate–MOF LJ cross interaction parameters by using the universal force field (UFF)[28] for the framework atoms. LJ potentials were truncated at 13 Å and electrostatic interactions between CO_2 molecules were truncated at 25 Å. Framework–CO_2 electrostatic interactions were calculated by summation of the charge–charge interactions between each framework atom and each charge site of CO_2. These charge–charge interactions were pre-tabulated by direct calculation of the atomic charge–charge interactions.[29] The charges on atoms in the MOF framework were determined by DFT calculations with Accelrys DMol,[3] employing the PWC functional within the local density approximation and a double numerical basis set.[30,31] These partial charges depend upon the charge partitioning method that is applied, so we assigned charges with both the Mulliken[32] and Hirshfeld[33] methods. The effect of these two sets of partial charges is discussed below.

A conventional GCMC technique was used to compute adsorption isotherms.[34] Simulations at the lowest fugacity for each system were started from an empty MOF. Each subsequent simulation at higher fugacity was started from the final configuration of the previous run. These simulations used 1.5×10^7 moves for equilibration and 1.5×10^7 moves for data collection at each state point. We report the adsorption isotherms as a function of fugacity. To convert fugacity into pressure, it would be necessary to use an equation of state to account for the non-ideality of CO_2 at the highest fugacities we simulated.

Fig. 2 shows the calculated single component and mixture adsorption isotherms of CH_4 and CO_2 in Cu(hfipbb)-(H_2hfipbb)$_{0.5}$ at room temperature. As in most MOFs, CO_2 is more strongly adsorbed than CH_4 because of the strong quadrupole moment of CO_2. Because interactions between CO_2 and the MOF are dominant at low loadings, the isotherms calculated with charges assigned from the Mulliken and Hirshfeld methods differ at pressures less than 0.1 bar. At higher pressures, however, adsorbate–adsorbate interactions are more dominant and the isotherms with the two sets of partial charges are similar. The single component adsorption isotherm of CH_4 reaches saturation at fugacities less than 1 bar. At these conditions, CH_4 is essentially an ideal gas, so fugacity and pressure are equivalent.

The mixture isotherm in Fig. 2 corresponds to equimolar bulk phase mixtures. As implied by the single component isotherms, CO_2 is favored over CH_4 in mixture adsorption. The adsorption selectivity for the equimolar bulk gas mixture is around 4 for the pressure range shown in Fig. 2. The observation that CO_2 is preferentially adsorbed in a MOF relative to CH_4 is not novel, and previous studies have shown that the adsorption selectivity is typically only weakly dependent on the bulk phase composition.[13,14,17,35]

Initial MD simulations of adsorbed CH_4 in Cu(hfipbb)-(H_2hfipbb)$_{0.5}$ indicated that CH_4 could not move between adjacent cages on the nanosecond time scales accessible using MD. The reasons for this behavior are clear from the potential energy surface for adsorbed CH_4. Fig. 3 shows that the minimum potential energy of CH_4 as the molecule is moved along a pore in the MOF. The minimum energy occurs in the

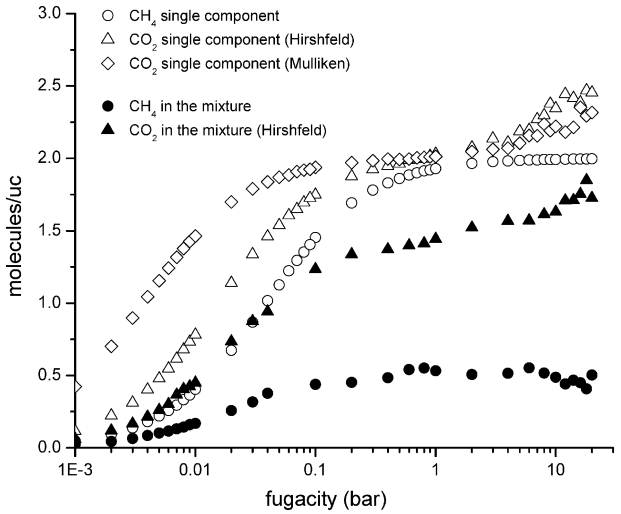

Fig. 2 Single component and mixture adsorption isotherms of CH_4 and CO_2 at 298 K in Cu(hfipbb)$(H_2$hfipbb$)_{0.5}$. Mixture isotherms are for an equimolar bulk phase mixture. For CO_2, results are shown with two different methods for assigning partial charges to the MOF framework atoms.

center of the MOF's cages, and these locations dominate adsorption of CH_4. A large energy barrier exists to moving CH_4 through the narrow windows connecting cages along the [010] direction; our calculations based on a rigid MOF structure give a barrier of $\Delta E \simeq 72$ kJ mol^{-1}. This corresponds to a diffusion coefficient that is far too slow to be directly observed with MD. We note that this approach could significantly underestimate the mobility of CH_4 if flexibility of the MOF's windows can lower the activation energy for diffusion. We examine this possibility later using quantum chemical calculations.

Unlike CH_4, CO_2 diffusion in Cu(hfipbb)$(H_2$hfipbb$)_{0.5}$ is rapid enough that it can readily be characterized using MD.

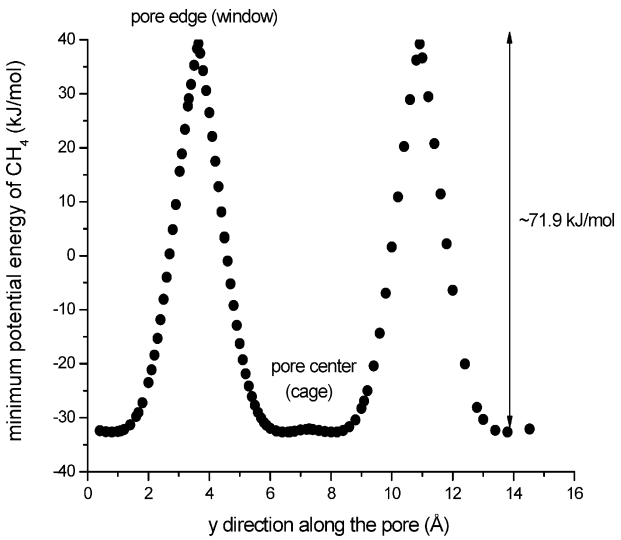

Fig. 3 Minimum potential energy of CH_4 as a function of position along the pore axis in Cu(hfipbb)$(H_2$hfipbb$)_{0.5}$, calculated using the methods described in the text.

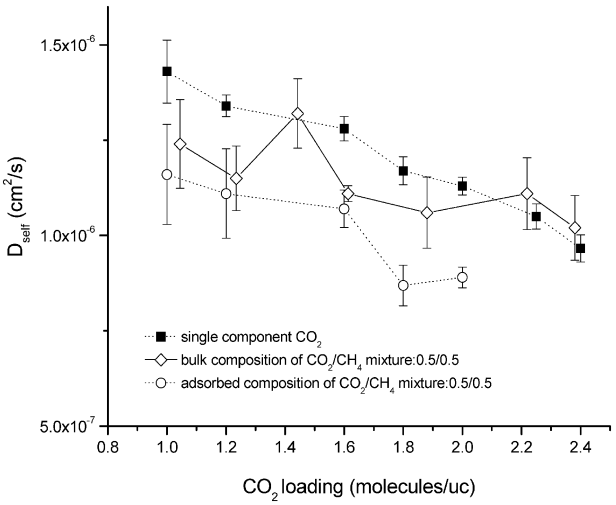

Fig. 4 Self diffusivities of CO_2 at 298 K in CO_2/CH_4 mixtures as a function of CO_2 loading at various compositions with single component diffusivity of CO_2 in Cu(hfipbb)$(H_2$hfipbb$)_{0.5}$.

We used EMD to compute the self diffusion coefficient of CO_2, both as a single component adsorbate and in adsorbed mixtures with CH_4. All MD calculations for CO_2 were performed using Hirshfeld charges; the results below are not sensitive to this choice. MD was performed in the canonical ensemble with a Nose-Hoover thermostat[34] for 20 independent MD simulations of length 20 ns for each loading and/or composition we considered. Initial states were created using GCMC, then equilibrated using a short EMD trajectory.

The computed self-diffusivities of CO_2 in Cu(hfipbb)-$(H_2$hfipbb$)_{0.5}$ are shown in Fig. 4. When CO_2 is adsorbed as a pure component, the self diffusivity is $\sim 10^{-6}$ cm^2 s^{-1} and decreases slightly as the adsorbate loading increases. As a benchmark, the diffusion coefficients of molecular solvents in liquids are typically $\sim 10^{-5}$ cm^2 s^{-1}. This result indicates that Cu(hfipbb)$(H_2$hfipbb$)_{0.5}$ satisfies the first property we listed above that is required for an effective kinetic separation because the diffusivity of one species (CO_2) is orders of magnitude larger than the other (CH_4).

The second requirement for an effective kinetic separation is that the presence of the slowly diffusing species must not significantly retard the rapidly diffusing species. There are many examples of nanoporous materials in which this undesirable slowing of motion is known,[36–38] so a general expectation is that this requirement will not be met. Fig. 4 shows the computed self diffusivity of CO_2 in 50/50 adsorbed CO_2/CH_4 mixtures. In every case, the diffusivity of CO_2 is reduced by less than a factor of 2 relative to pure CO_2. The origin of this desirable effect is easy to understand; CO_2 and CH_4 molecules can readily pass one another in the cages of the MOF. The presence of the slowly moving CH_4 molecules has at most a weak impact on the net diffusion of CO_2.

A complication with the binary data discussed above is that it is defined in terms of the adsorbed mixture concentration, which obscures the diffusion properties of mixtures that are relevant for typical gas compositions. Fig. 4 also shows results for the adsorbed mixture associated with an equimolar bulk mixture. Because of the adsorption selectivity of the MOF

(*cf*. Fig. 1), the adsorbed mixture in this case is $\sim$80% CO_2. The diffusivity of CO_2 in these adsorbed mixtures is only slightly smaller than the result for pure CO_2.

Our molecular simulations predict that Cu(hfipbb)-$(H_2$hfipbb$)_{0.5}$ has excellent properties for a membrane-based separation of CO_2 from CO_2/CH_4 mixtures, since adsorption favors CO_2 by a moderate factor and diffusion favors CO_2 by orders of magnitude. Because this desirable outcome rests heavily on the large activation barrier that was calculated for CH_4 diffusion using a rigid MOF structure, it is important to understand whether allowing flexibility in the MOF structure will significantly reduce this barrier. Because the development of accurate classical force fields for the internal degrees of freedom in MOFs is challenging,[12,39] addressing this topic with molecular simulations is problematic. As in small pore zeolites,[18] the large barrier that exists for CH_4 diffusion through the windows of Cu(hfipbb)$(H_2$hfipbb$)_{0.5}$ is dominated by short-range repulsive interactions, not long range dispersion forces. This means that DFT calculations can be used to reliably probe these interactions. We have therefore used plane wave DFT calculations to examine the effect of MOF flexibility on the diffusion of CH_4 in Cu(hfipbb)$(H_2$hfipbb$)_{0.5}$.

We used the Vienna *ab initio* Simulation Package (VASP)[40] for our DFT calculations. The computational supercell is fully periodic in all directions, and represents the full crystal structure of the MOF. The PW91 GGA functional[31] was used to describe electron exchange-correlation with a kinetic energy cutoff of 500 eV and a $1 \times 2 \times 1$ Monkhorst-Pack sampling of *k*-space.[41] Geometry optimizations were performed until the maximum force on each atom was $<3 \times 10^{-2}$ eV Å^{-1}. Spin polarization was included to consider the MOF's magnetic ground state; we determined that the Cu dimers are antiferromagnetically coupled as they are in other MOFs such as CuBTC.[42,43] The experimental crystal structure of Cu(hfipbb)-$(H_2$hfipbb$)_{0.5}$ from Pan *et al*.[24] was used in all DFT calculations, holding the cell parameters fixed. This choice is appropriate because the rare event associated with CH_4 moving through a window is unlikely to affect the net lattice parameters. Only the 6 C and 4 H atoms in each ring associated with the pore window were allowed to relax during our calculations; all other atoms in the MOF were constrained in their crystallographic positions. The degrees of freedom of the adsorbate molecules were chosen depending on the type of the calculation as described below.

Adsorption energies of CO_2 and CH_4 in the pore of Cu(hfipbb)-$(H_2$hfipbb$)_{0.5}$ were calculated after relaxation of each molecules in the cage of the MOF. All degrees of freedom in the adsorbates and the aromatic rings in the MOF mentioned above were allowed to relax in these calculations. The adsorption energy is given by

$$E_{ads} = E(\text{MOF} + \text{adsorbate}) - E(\text{MOF}) - E(\text{adsorbate}),$$

where E(MOF + adsorbate), E(MOF), and E(adsorbate) are the total energies of the MOF with an adsorbate molecule, the MOF with no adsorbate, and an isolated adsorbate molecule, respectively. The results are shown in Table 1. We anticipate that our DFT calculations strongly underestimate the attractive dispersion forces that exist for each molecule inside the MOF.[44,45] When the molecules are adsorbed in the MOF's cage, they each give DFT adsorption energies that are slightly negative (see Table 1). Within the caveat above regarding dispersive interactions, this result is qualitatively consistent with the experimental observation of Pan *et al*. that alkanes adsorb readily in the MOF.[24]

Table 1 Adsorption energies in the cage, diffusion activation energy and rotation angles of aromatic rings in the window for CO_2, CH_4, and C_2H_6

	CO_2	CH_4	C_2H_6
E_{ads} (kJ mol^{-1})	−9.7	−5.8	0.0
E_{trans} (kJ mol^{-1})	16	45	45
Mean rotation angle (deg.)	2.4	4.3	5.8

The activation energies for CO_2 and CH_4 diffusion were estimated by constraining the C atom in each molecule in the center of the MOF's window and allowing the remaining adsorbate degrees of freedom and the aromatic rings described above to relax. This is a rather crude way to determine the transition barrier but because of the simple geometry of the system it is sufficient to distinguish differences in the activation barrier between these adsorbates. Repeating this calculation with the positions of the adsorbate's C atoms shifted by $\pm$1.0 Å along the pore axis support the identification of the window as a transition state. The diffusion activation energy is defined as the difference in the total energies of a molecule in the window and in the pore, $E_{trans} = E_{window} - E_{pore}$. As shown in Table 1, the activation energy for CH_4 is computed to be 45 kJ mol^{-1}, compared with 16 kJ mol^{-1} for CO_2. In the estimated transition states, the aromatic rings of the framework rotate by a small amount (2.4° for CO_2 and 4.3° for CH_4) relative to the rigid structure. Using DFT without relaxation of these rings gave a CH_4 activation energy of 57 kJ mol^{-1}. This value is smaller than the 72 kJ mol^{-1} predicted by our molecular simulation, but it is clear that the activation energy for CH_4 diffusion in this MOF is much larger than for CO_2, and that including flexibility in the MOF does not change this qualitative conclusion.

To compare our DFT calculations more directly with the experiments of Pan *et al*. with adsorbed alkanes, we performed similar calculations for C_2H_6. To estimate the transition state for C_2H_6 diffusion, both C atom positions were fixed with the C–C bond along the pore axis, while all adsorbate H atoms were allowed to move. The calculated diffusion activation energy for C_2H_6 is identical to that of CH_4 within the accuracy of our calculations. This is reasonable considering that passage of C_2H_6 through the window is dominated by the energy required to place a single methyl group in the pore window. This implies that the activation energy for propane and butane to diffuse in Cu(hfipbb)$(H_2$hfipbb$)_{0.5}$ is likely to be similar to that of CH_4.

We can use a simple transition state expression to estimate the diffusivity of CH_4 in Cu(hfipbb)$(H_2$hfipbb$)_{0.5}$ by assuming that the CH_4 hopping rate between cages is $k = \nu\exp(-E_{trans}/k_BT)$. Taking the pre-exponential to be $\nu = 10^{12}$–10^{13} s^{-1} implies that the average time between cage-to-cage hops is 0.7–7 μs, using our DFT result for the activation energy. This gives

a one-dimensional diffusivity, $D = \frac{1}{2}ka^2$, of 0.4–4 $\times$ 10^{-10} cm^2 s^{-1}, where $a = 0.727$ nm is the cage-to-cage distance along the pore. This value is comparable to the diffusion coefficient of many bulky molecules in zeolites; the self diffusivity of benzene in Na-X, for example, is $\sim 10^{-10}$ cm^2 s^{-1}.[46] Even though this diffusion is slow relative to CO_2, it is easily high enough that well equilibrated samples could be observed in the alkane adsorption experiments of Pan *et al*. We can therefore conclude that our calculations are consistent with all features of these experiments.

A simple estimate of the selectivity of a membrane for a binary mixture of CO_2 and CH_4 is given by $S_{CO_2/CH_4} = \frac{c_{CO_2}}{c_{CH_4}}\frac{D_{CO_2}}{D_{CH_4}}$, where c_i (D_i) is the adsorbed amount (diffusivity) of species i in the adsorbed mixture of interest. Our calculations predict that $c_{CO_2}/c_{CH_4} \sim 4$ for a broad range of bulk phase compositions. Our MD simulations indicate that the diffusivities of the two species in adsorbed mixtures are quite similar to the diffusivities of the pure adsorbed components, so it is reasonable to estimate D_{CO_2}/D_{CH_4} using pure component values. Using our MD results for the rapidly diffusing CO_2 and the transition state theory (TST) estimate with a DFT-based activation energy for CH_4, we predict that $D_{CO_2}/D_{CH_4} \sim 2400$–$24\,000$. That is, our calculations predict that a membrane based on this MOF would have a net selectivity for CO_2 of 10^4–10^5. This selectivity is higher than any known polymeric membrane for this separation[47] or the high performance zeolite membranes that have been developed recently.[20,48] In polymeric membranes, high selectivity is almost inevitably associated with low permeability.[49] This tradeoff will not be present for Cu(hfipbb)$(H_2$hfipbb$)_{0.5}$ membranes, where the relatively high diffusion coefficient of CO_2 will lead to high permeabilities, as in other MOF membranes with larger pores.[13]

Our results present a compelling motivation to fabricate and test membranes incorporating Cu(hfipbb)$(H_2$hfipbb$)_{0.5}$ experimentally. The analysis above was based upon a membrane made entirely from the MOF. The possibility of fabricating MOF membranes of this kind has already been demonstrated with another MOF.[50] A second application of Cu(hfipbb)-$(H_2$hfipbb$)_{0.5}$ would be as a dispersed component in a polymeric membrane. These so-called mixed matrix membranes (MMMs) offer a useful avenue for tuning the properties of polymeric membranes, thus leveraging the commercial technologies that already exist for making high surface area membranes. Initial studies of MMMs with large pore MOFs[16,51] have indicated that MOFs are relatively straightforward to incorporate into these membranes.

In addition to identifying a specific MOF predicted to have extraordinary properties as a membrane for an industrially important separation, our results hint that multiple other MOFs with excellent properties for kinetic separations also exist. We have demonstrated that a well developed suite of computational methods can be used to examine molecular adsorption and diffusion in MOFs in a way that should open exciting opportunities for developing materials for these kinds of applications.

SK and DSS received partial support from the NSF (CTS-0413027 and CTS-0556831).

References

1 F. G. Kerry, *Industrial Gas Handbook: Gas Separation & Purification*, CRC Press, Boca Raton, FL, 2007.
2 W. J. Koros and R. Mahajan, *J. Membr. Sci.*, 2000, **175**, 181.
3 N. J. Themelis and P. A. Ulloa, *Renewable Energy*, 2007, **32**, 1243.
4 A. J. Kidnay and W. R. Rarrish, *Fundamentals of Natural Gas Processing*, CRC Press, Boca Raton, 2006.
5 B. Metz, O. Davidson, H. de Coninck, M. Loos and L. Meyer, *IPCC Special Report on Carbon Dioxide Capture and Storage*, Cambridge University Press, Cambridge, 2005.
6 R. W. Baker, *Membrane Technology and Applications*, Wiley, Chichester, England, 2004.
7 J. L. C. Rowsell and O. M. Yaghi, *Microporous Mesoporous Mater.*, 2004, **73**, 3.
8 O. M. Yaghi, M. O'Keeffe, N. W. Ockwig, H. K. Chae, M. Eddaoudi and J. Kim, *Nature*, 2003, **423**, 705.
9 G. Garberoglio, A. I. Skoulidas and J. K. Johnson, *J. Phys. Chem. B*, 2005, **109**, 13094.
10 S. Wang, Q. Yang and C. Zhong, *Sep. Purif. Technol.*, 2008, **60**, 30.
11 J. A. Greathouse, T. L. Kinnibrugh and M. D. Allendorf, *Ind. Eng. Chem. Res.*, 2009, **48**, 3425.
12 S. Keskin, J. Liu, R. B. Rankin, J. K. Johnson and D. S. Sholl, *Ind. Eng. Chem. Res.*, 2009, **48**, 2355.
13 S. Keskin and D. S. Sholl, *J. Phys. Chem. C*, 2007, **111**, 14055.
14 S. Keskin and D. S. Sholl, *Ind. Eng. Chem. Res.*, 2009, **48**, 914.
15 S. Keskin, J. Liu, J. K. Johnson and D. S. Sholl, *Microporous Mesoporous Mater.*, 2009, **125**, 101.
16 E. V. Perez, K. J. Balkus, J. P. Ferraris and I. H. Musselman, *J. Membr. Sci.*, 2009, **328**, 165.
17 S. Keskin and D. S. Sholl, *Langmuir*, 2009, **25**, 11786.
18 S.-E. Jee and D. S. Sholl, *J. Am. Chem. Soc.*, 2009, **131**, 7896.
19 T. Tomita, K. Nakayama and H. Sakai, *Microporous Mesoporous Mater.*, 2004, **68**, 71.
20 S. G. Li, J. L. Falconer and R. D. Noble, *Adv. Mater.*, 2006, **18**, 2601.
21 S. G. Li, J. L. Falconer and R. D. Noble, *J. Membr. Sci.*, 2004, **241**, 121.
22 L. Pan, M. B. Sander, X. Y. Huang, J. Li, M. Smith, E. Bittner, B. Bockrath and J. K. Johnson, *J. Am. Chem. Soc.*, 2004, **126**, 1308.
23 J. Y. Lee, J. Li and J. Jagiello, *J. Solid State Chem.*, 2005, **178**, 2527.
24 L. Pan, D. H. Olson, L. R. Ciemnolonski, R. Heddy and J. Li, *Angew. Chem., Int. Ed.*, 2006, **45**, 616.
25 W. Zhu, F. Kapteijn, J. A. Moulijn, M. C. den Exter and J. C. Jansen, *Langmuir*, 2000, **16**, 3322.
26 J. G. Harris and K. H. Yung, *J. Phys. Chem.*, 1995, **99**, 12021.
27 S. Y. Jiang, K. E. Gubbins and J. A. Zollweg, *Mol. Phys.*, 1993, **80**, 103.
28 A. K. Rappe, C. J. Casewit, K. S. Colwell, W. A. Goddard and W. M. Skiff, *J. Am. Chem. Soc.*, 1992, **114**, 10024.
29 A. I. Skoulidas and D. S. Sholl, *J. Phys. Chem. B*, 2005, **109**, 15760.
30 B. Delley, *J. Chem. Phys.*, 2000, **113**, 7756.
31 J. P. Perdew and Y. Wang, *Phys. Rev. B: Condens. Matter*, 1992, **45**, 13244.
32 R. S. Mulliken, *J. Chem. Phys.*, 1955, **23**, 1833.
33 F. L. Hirshfeld, *Theor. Chim. Acta*, 1977, **44**, 129.
34 D. Frenkel and B. Smit, *Understanding Molecular Simulation: From Algorithms to Applications*, Academic Press, San Diego, 2nd edn, 2002.
35 Q. Yang and C. Zhong, *J. Phys. Chem. B*, 2006, **110**, 17776.
36 D. S. Sholl, *Acc. Chem. Res.*, 2006, **39**, 403.
37 R. Krishna and D. Paschek, *Phys. Chem. Chem. Phys.*, 2002, **4**, 1891.
38 D. Paschek and R. Krishna, *Phys. Chem. Chem. Phys.*, 2001, **3**, 3185.
39 J. A. Greathouse and M. D. Allendorf, *J. Phys. Chem. C*, 2008, **112**, 5795.
40 G. Kresse and J. Furthmuller, *Phys. Rev. B: Condens. Matter*, 1996, **54**, 11169.
41 H. J. Monkhorst and J. D. Pack, *Phys. Rev. B: Solid State*, 1976, **13**, 5188.

42 A. Poppl, S. Kunz, D. Himsl and M. Hartmann, *J. Phys. Chem. C*, 2008, **112**, 2678.
43 X. X. Zhang, S. S. Y. Chui and I. D. Williams, *J. Appl. Phys.*, 2000, **87**, 6007.
44 J. Hafner, *J. Comput. Chem.*, 2008, **29**, 2044.
45 A. J. Cohen, P. Mori-Sanchez and W. T. Yang, *Science*, 2008, **321**, 792.
46 F. J. Keil, R. Krishna and M. O. Coppens, *Rev. Chem. Eng.*, 2000, **16**, 71.
47 L. M. Robeson, *J. Membr. Sci.*, 2008, **320**, 390.
48 M. A. Carreon, S. G. Li, J. L. Falconer and R. D. Noble, *J. Am. Chem. Soc.*, 2008, **130**, 5412.
49 L. M. Robeson, *J. Membr. Sci.*, 1991, **62**, 165.
50 Y. Liu, Z. Ng, E. A. Khan, H.-K. Jeong, C.-B. Ching and Z. Lai, *Microporous Mesoporous Mater.*, 2009, **118**, 296.
51 Y. Zhang, I. H. Musselman, J. P. Ferraris and K. J. Balkus, *J. Membr. Sci.*, 2008, **313**, 170.

